

Semi-quantitative landslide risk assessment using GIS-based exposure analysis in Kuala Lumpur City

Omar F. Althuwaynee & Biswajeet Pradhan

To cite this article: Omar F. Althuwaynee & Biswajeet Pradhan (2017) Semi-quantitative landslide risk assessment using GIS-based exposure analysis in Kuala Lumpur City, Geomatics, Natural Hazards and Risk, 8:2, 706-732, DOI: [10.1080/19475705.2016.1255670](https://doi.org/10.1080/19475705.2016.1255670)

To link to this article: <https://doi.org/10.1080/19475705.2016.1255670>



© 2016 The Author(s). Published by Informa UK Limited, trading as Taylor & Francis Group



Published online: 02 Dec 2016.



Submit your article to this journal [↗](#)



Article views: 3661



View related articles [↗](#)




View Crossmark data [↗](#)



Citing articles: 20 View citing articles [↗](#)

Semi-quantitative landslide risk assessment using GIS-based exposure analysis in Kuala Lumpur City

Omar F. Althuwaynee ^{a,b} and Biswajeet Pradhan ^{a,c}

^aFaculty of Engineering, Department of Civil Engineering, Geospatial Information Science Research Center (GISRC), University Putra Malaysia, Serdang, Selangor Darul Ehsan, Malaysia; ^bFaculty of Engineering and Architecture, Department of Geomatics Engineering, Izmir Katip Celebi University, Cigli, Izmir, Turkey; ^cDepartment of Energy and Mineral Resources Engineering, Choongmu-gwan, Sejong University, 209 Neungdong-ro Gwangjin-gu, Seoul, Republic of Korea

ABSTRACT

A semi-quantitative landslide-risk assessment method, which would provide a spatial estimate of future landslide risks in a densely populated area in Kuala Lumpur City, was presented in this study. This work focused on detail risk assessment by identifying the number of elements at risk. A medium-scale analysis was performed using geospatial based techniques. The estimation of rainfall threshold and the landslide hazard map used in the current work are obtained from the previous literature published by the same authors. Subsequently, the vulnerability value was generalized, and then a valid integration between elements at risk and the hazard map was conducted to determine the expected number of elements that would likely be under direct risk. Results showed that the approximate number of predicted affected elements per pixel, as a percentage of the settlement unit, is nearly 50% in residential areas, 35% in commercial buildings, 31% in industrial buildings, 31% in utility areas, and 18% in densely populated areas. Similarly, a significant percentage of predicted losses (27%) were found for the road network. The results showed the capability of the method to approximately predict the number of infrastructure elements and the population density under landslide risk in data-scarce environments.

ARTICLE HISTORY

Received 25 June 2016
Accepted 27 October 2016

KEYWORDS

Landslide; risk assessment; GIS; vulnerability; hazard; remote sensing; Malaysia

1. Introduction

Landslides have devastating effects worldwide, as evidenced by the 200,000 casualties recorded from the 25 most catastrophic landslides in the twentieth century (Schuster 1996; Carrara et al. 2003; Crozier & Glade 2006; Lee 2007; Schlögel et al. 2011). A landslide causes serious economic damage, particularly in highly dense urban areas; fallen rocks obstruct highways and sub-roads in urban regions. Recently, the death toll has dramatically increased as a result of global and micro climate change, the incremental increase in population, and the ever-expanding road networks. Quantifying economic losses, particularly of severely affected rural communities in remote areas, is generally difficult (Sassa & Canuti 2008).

Landslide hazard is the probability of occurrence of a potentially damaging landslide of a given magnitude within a specified period (temporal) and area (spatial) (Glade et al. 2005). Landslide risk indicates possible losses that may be incurred within a specific period (Erener & Düzgün 2013). Varnes and the International Association of Engineering Geology Commission on Landslides and Other

Mass Movements on Slopes (1984) defined risk as the expected loss of life (including injuries) and the losses to property and economy, in general, particularly in terms of spatio-temporal reference. Quinn et al. (2011) observed that precautions for indirect hazards were frequently weak or neglected. For example, damage to railway tracks may be considered a direct effect of hazard, whereas substantial economic losses resulting from damage to an entire railway network system may be considered indirect effects. Damages to gas transmission lines may also result in substantial economic losses, particularly when the network exhibits minimal redundancy, such that service disruptions cannot be mitigated by rerouting gas delivery.

Risk assessment comprises three main parts (Bell & Glade 2004; Sidle & Ochiai 2006). First, risk analysis refers to the process based on geotechnical engineering methods that are performed to determine risk in a certain environment. Second, risk evaluation is a method for identifying risk perception and the acceptance of the level of threat of certain elements at risk. Third, risk management involves the final decision on mitigation planning and effective precautionary procedures (Sidle & Ochiai 2006).

van Westen et al. (2006) classified hazard assessment into four approaches (Table 1). The first is the landslide inventory-based probabilistic approach, which addresses the direct exposure of a single slope failure and its consequences. The second is the heuristic approach (e.g. direct geomorphological mapping or indirect combination of qualitative maps), which is mainly regarded as a qualitative and semi-quantitative assessment method that relies on expert opinion. The third is the statistical approach (bivariate or multivariate statistics-based method), which is preferable for all types of susceptibility and hazard assessments. The fourth is the deterministic approach, which is a quantitative-based method (Wang et al. 2005).

Geomorphological analyses typically stop at the hazard assessment stage. Only a few attempts have proceeded to qualitative or quantitative risk assessment (Glade 2003), thereby reflecting the difficulties in obtaining data on past losses and assessing future losses.

Sidle and Ochidi (2006) suggested that two basic approaches could be used in risk assessment. The quantitative approach yields direct and countable results but is limited by data availability. By contrast, the qualitative approach is less complex, but the subjective estimation of experts renders its degree of confidence and the accuracy of its results questionable.

Quantitative risk analysis (QRA) at the regional scale was presented in Catani et al. (2005) to provide a mean annual risk without information on the expected distribution of annual costs. Recently, applications of regional-scale QRA that provided exceedance probabilities were presented in Jaiswal et al. (2011). Although most QRA methodologies have been developed for local or regional scales, some of them, such as the approach proposed in Catani, et al. (2005), may be applied to a larger area (Nicolet et al. 2013). Remondo et al. (2008) developed an approach based on the analysis of the spatio-temporal distribution of landslides and the corresponding damages during a period of nearly 50 years by assuming the uniformitarian behaviour of slope processes.

Promper et al. (2015) studied the application of a scenario-based approach for regional future landslide exposure assessments based on the physical location of hazardous phenomena, the elements at risk, and their relocation over time as land-cover changes.

The primary components of landslide risk analysis and assessment (Equation (1)) include hazard, vulnerability, and elements at risk (Varnes 1984). Some authors have included the frequency of

Table 1. Usefulness of specific combination of hazard approaches and risk approaches for GIS-based landslide risk zonation at medium scale. The combinations are indicated with a number from 0 (not useful) to 3 (most useful) (van Westen et al. 2006).

Hazard approaches	Risk approaches		
	Qualitative	Semi-quantitative	quantitative
Inventory-based probabilistic approach	2	2	2
Heuristic/geomorphological/direct mapping/expert-based approach	3	3	0
Statistical approach (bivariate or multivariate)	3	2	2
Deterministic and dynamic modelling approach	0	1	3

occurrence of a disaster scenario during hazard assessment in terms of time recurrence or probability:

$$\text{Risk} = \text{Hazard} \times \text{Vulnerability} \times \text{Elements at risk} \quad (1)$$

Vulnerability determines the degree of loss for elements (utilities, road networks, people) within the affected area of the landslide hazard (Fell 1994). Vulnerability assessment is a complex task (Pazzi et al. 2016) because it may include social, political, and physical elements. Uncertainties on the completeness, quality, and reliability of raw data on damages may occur. Establishing the relationship between the elements that will be affected in the future and the unknown landslide intensity is extremely difficult. By contrast, semi-quantitative assessment provides a general view of the relative importance of future damages. Thus, the existing literature contains few articles that deal with stochastic-based approaches. These approaches have been mostly applied in assessing vulnerability by adopting source data with various resolutions (Fell 1994; Li et al. 2010).

Risk losses may be economic, social and human, or environmental. Economic losses result from damages to roads and infrastructure, including failure of utility lines, leakage in irrigation ditches, erosion, underground water problems, rock falls, and sinkholes (Glade, et al. 2005). Details regarding the main advantage of risk assessment are provided in Das (2011).

Some studies (Corominas & Moya 2008; Lu et al. 2014) considered expected annual loss as the main risk measurement, depending on the cost of construction of the elements at risk before landslide occurrence and the cost of rehabilitation or cost of remedy after landslide occurrence. In Equation (2), landslide risk is directly related to deforestation in prone areas and to increments in triggering factors, such as heavy precipitation and seismic activities (Armaş 2014):

$$R(P) = \sum_{i=1}^K [P(L_i) \times P(T : L) \times V(D_i)] \times C, \quad (2)$$

where $R(P)$ is the expected annual loss (€/yr), $P(L_i)$ is the annual probability of occurrence with magnitude i , $P(T:L)$ is the probability of a landslide that is likely to affect the element at risk, $V(D_i)$ is the vulnerability of the element at risk, and C is the cost of the building.

The Pacific Disaster Center, in collaboration with several organizations in Asia and the Pacific, has established a risk and vulnerability assessment programme to assess the effect of landslides on local communities. Glade (2003) and Roberds (2005) showed that no clear and unique framework existed for risk assessment because of the complexity of temporal variability and the difficulties and constraints that limited spatio-temporal modelling. Trigila et al. (2010) classified risk assessment with respect to landslide categories: rapid movement (in terms of human lives and properties) and slow movement (in terms of utilities and infrastructure).

In a data-scarce environment, Ghosh et al. (2012) followed the assumption that all elements at risk would be equally vulnerable to landslides. In determining the risk related to each zone, they used the average value of the population density for the population damage and the maximum number of expected vehicles at any moment in time. Then, the elements at risk were transformed into a probability using the sigmoid curve equation for property value and the Poisson curve equation for population density (Ghosh et al. 2012). The exposure-based approach (Lee & Jones 2004) for rock-fall hazards estimated the likelihood of pixels being occupied by elements at risk and the potential losses related to the expected event. Ghosh et al. (2012) used 12 landslide hazard scenarios to calculate the number of elements at risk. They concluded that the exposure-based approach would be capable of identifying the number of buildings, population density, and road network at risk for the preparation of risk maps despite a data-scarce environment.

From the aforementioned literature review, minimal work has been conducted on comprehensive landslide risk (beyond hazard) analysis in Malaysia. This gap is mostly attributed to the

unavailability of complete data-sets related to socio-economic factors. Thus, the main objectives of the current study are to focus on identifying the elements under exposure and to determine the vulnerability of risk (specifically for land uses, road networks, and population) that will result from future landslides in Kuala Lumpur City, Malaysia. A semi-quantitative risk assessment method was chosen because of limitations in socio-economic data resources related to landslide risk losses, which reflected negatively in generalizing the vulnerability value. The achievements of the proposed semi-quantitative risk mapping are expected to help concerned authorities improve the efficiency of land-use planning.

In the current study, a structural analysis or an overview on potential building damages, as well as the safety factor of different structure types (single- and double-storey houses or apartments), is not available. In addition, the types of foundations and slope embankments are incomplete and generally unavailable. Guikema (2009) presented specific assumptions that should be followed to enhance theory of construction design in hazardous areas, such as (1) improving the design stage (e.g. cost-benefit relationship in different design alternatives), (2) determining the level of robustness of a design (e.g. contaminant releases, degradation of ecosystems), and (3) considering natural modes of ecosystem protection (e.g. design of a levee).

2. Study area

Kuala Lumpur is the federal and economic capital of Malaysia and it is located in Selangor State. It has six strategic zones according to the Kuala Lumpur City Hall Government Agency, namely Sentul Menjalara, Wangsa Maju Maluri, Damansara Penchala, Bukit Jalil Seputeh, Bandar Tun Razak Sg. Besi, and Pusat Bandar Raya (arranged from the largest to smallest), which cover a total area of 242.8 km² (Table 2). The landform of the area ranges from very flat terrain (particularly for the peat swamp forest), abandoned mining area, grassland, and scrub area, to hilly regions ranging from 0 to 420 m above sea level (Lee & Pradhan 2007). The area receives its highest temperatures (between 29 and 32 °C registered) from April to June, and the average relative humidity is from 65% to 70% throughout the year except in June, July, and September (Malaysian Meteorological Services Department). Rainfall is the main triggering factor for the initiation of landslides, and precipitation averages from 58 to 240 (mm/month). When the area receives a high amount of rainfall, infiltration results, thereby causing water to enter the soil from its surface (Xie et al. 2004).

Kuala Lumpur City suffers from frequent landslides, particularly along the western zone (Damansara Penchala zone) and the north-western zone (Sentul Menjalara zone), which cover a combined area of 107.3 km² (Figure 1). The farthest sections of the south-western zone of Damansara Penchala and the north-western zone of Sentul Menjalara are characterized by high-steep slopes and semi-rural areas with dense vegetation cover. These areas experience several slope failures throughout the year. The steepness of slope angles in the area may reach 50°, particularly in the Damansara Penchala zone.

The average monthly precipitation rate from 2000 to 2012 was 237 mm. Althuwaynee et al. (2015, 2012) reported that the study area received an average daily rainfall of 20–50 mm during its two monsoon seasons. The south-west monsoon starts from May to September, followed by the north-east monsoon from November to March. For the rest of the year, the average daily rainfall is between 10 and 25 mm.

Table 2. Statistics summary.

Zone	Area (km ²)	Population (hab.)	Density (person/km ²)
Kuala Lumpur	242.8	1,627,172	6696
Sentul Menjalara (SM)	54.8	345,295	6301
Damansara Penchala (DP)	52.5	148,668	2831

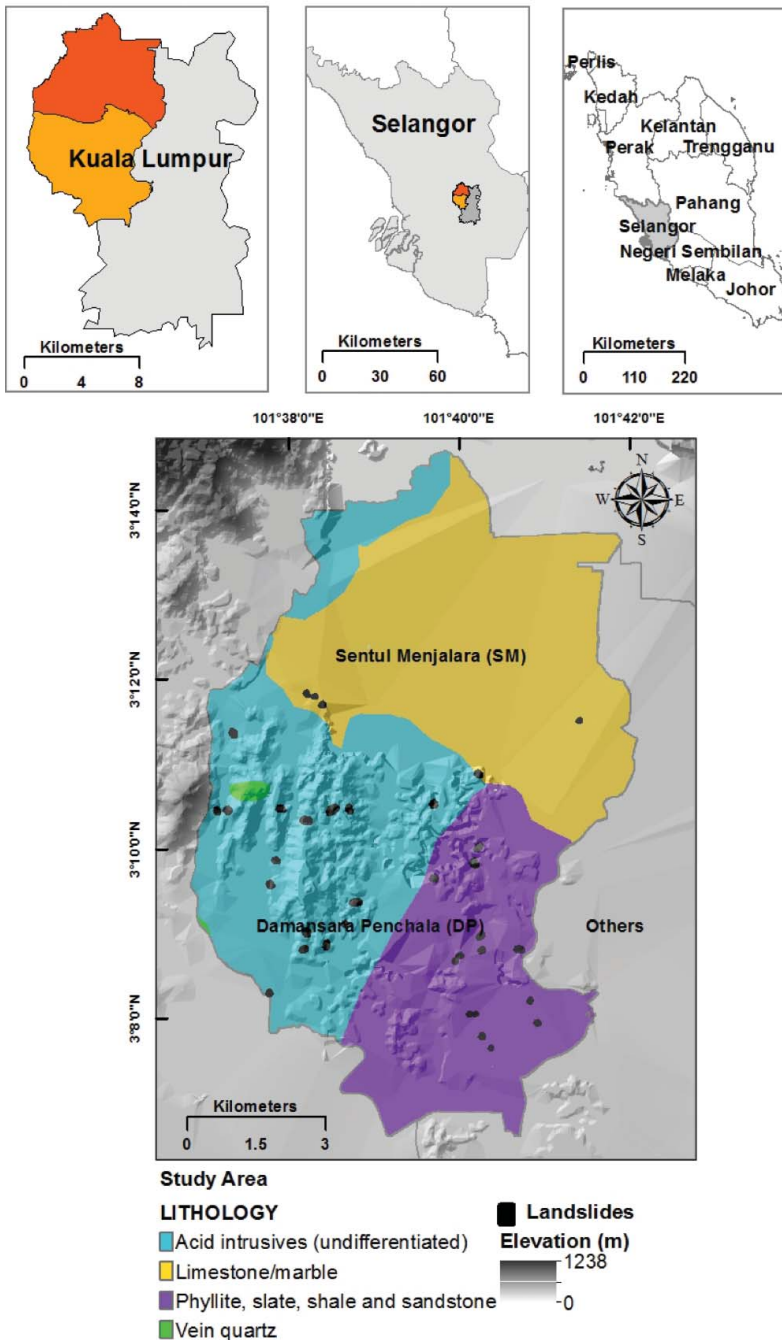


Figure 1. Simplified geological map of the two study areas of Kuala Lumpur.

The area is generally underlain by granitic rock, phyllite and schist, and limestone with minor intercalations of phyllite. Most of the historical landslides occurred on the granitic rock formation. The weathering of granitic rock produced Grades V and VI sandy silt residual soil with a thickness of approximately 15–30 m (Lee et al. 2014). The deposit of granitic residual soil layer produced by

different degrees of the weathering process leads to large variations in engineering properties and contributes positively to creating a variety of mechanical soil behaviour. The only comprehensive publication available on the geology of Peninsula Malaysia is by Hutchison (1975). However, the Geological Survey Department periodically publishes and updates detailed maps and reports. Notably, the saturated coefficient of hydraulic conductivity within a residual soil layer may vary for up to two orders of magnitude in some cases, thereby leading to uncertainty in the hydraulic responses of soil slope to water infiltration (Lee et al. 2014).

In this study, shallow rotational medium-scale landslides were used in the analysis. The majority of these landslides have occurred at cut slopes, road embankments, and highways. In December 1993, a catastrophic landslide occurred in granitic formation in Taman Hill view, Ulu Klang, which caused 48 deaths and collapsed the Highland Towers. In May 1999, another major debris flow occurred in the meta-sediment formation in Bukit Antarabangsa, Ulu Klang which, killed few people and injured the local residents.

Urban areas represent the major part of the land cover that historically and periodically passes through systematic forest cutting and logging activities. Tin mining has a long history in the study area and many abandoned mines have been converted into residential areas. Tectonically, the Selangor area forms part of the Sunda Shield. Its folded mountain system exhibits the dominant regional trend from northerly to north-westerly. Geological formations range from the Cambrian to the Quaternary. The main rocks are pre-Triassic and post-Triassic. In general, pre-Triassic rocks have both marine and non-marine origins, whereas post-Triassic rocks are characteristically non-marine and found in the Upper Triassic layer. Four major episodes of granite emplacement, which reflect the relationship among known mineralization events, occurred because of faulting. The majority of known mineralization events occurred during later episodes and was commonly associated with faulting. Cliffs and high-slope areas are composed of limestone, with vegetation surviving on a thin layer of topsoil. Limestone is the main source of building and construction materials in the study area. Hence, limestone quarries pose a significant negative effect on the stability of soil layers (Althwaynee et al. 2012).

3. Materials and methods

3.1. Data

The data covered two zones of Kuala Lumpur: the western (Damansara Penchala) and northern (Sentul Menjalara) parts. The data-set includes land uses (commercial, industrial, utilities, and residential) and road networks based on a 2013 master plan, as well as a 2010 census map of population density. The total study area was measured using a virtual fishnet square grid. Moreover, the net cells represented the settlement units (SUs) in the land-use map. A mesh was produced to resemble the total study area, with each cell covering an area of 250 m × 250 m (de Noronha Vaz et al. 2011).

Each SU was characterized by the attributes of residential buildings (Figure 2(a)), including the total number and type of residential structures (single- and double-storey houses, condominiums, and apartments), which represented the largest land-use settlement (25%). The land-use map (Figure 2(b)) shows commercial (3%) and industrial areas (3%), as well as utility areas (1%). The rest of the study area comprises institutions, graveyards, public facilities, squatter settlements, and open spaces. Moreover, 16% of the study area was underdeveloped. Squatters occupied over 1.7 km² of the study area, particularly along the western and eastern regions of Sentul Menjalara. Squatter settlements reflect the uncontrolled urban sprawl, which results from the lack of awareness in building design styles, particularly in landslide-prone areas.

The population density map (Figure 2(c)) was prepared based on the 2010 census from the Department of Statistics. The road network (highways, secondary roads, and corridors) map was prepared and functionally categorized to calculate direct loss for each category using the unit of length (Figure 2(d)).

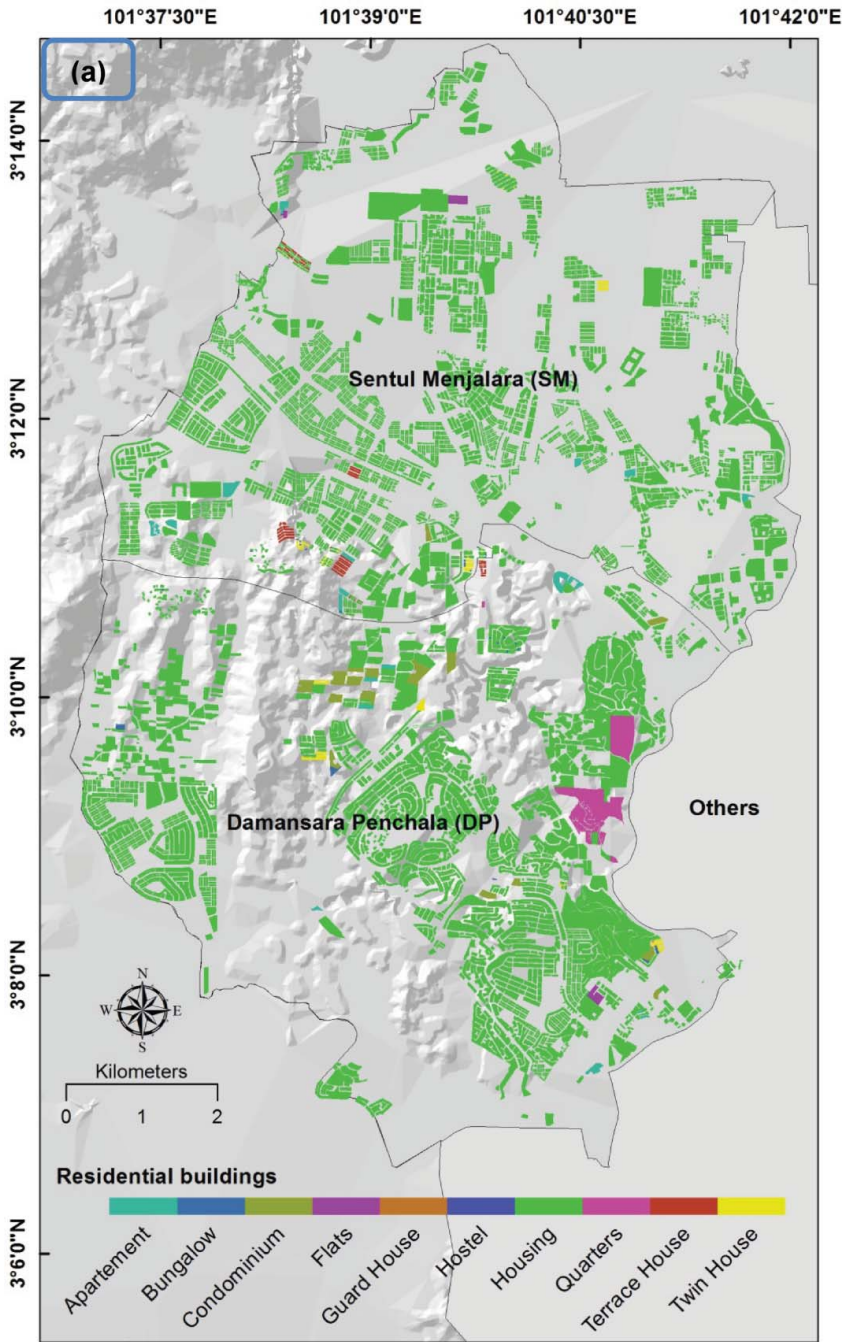


Figure 2. Elements-at-risks of the study area: (a) residential buildings; (b) commercial, industrial buildings and utilities areas; (c) population density (hab./km²); and (d) roads network.

Notably, the wide spectrum of literature (books, articles, site reports, and local press news) emphasizes the economic and ecological losses in the study area (Jamaludin & Hussein 1993; McInnes 2007; Sassa & Canuti 2008) without referring to exact or long-term records. A list of the most devastating landslides that occurred around Selangor can be found in the previously published article of the author (Althuwaynee et al. 2012).

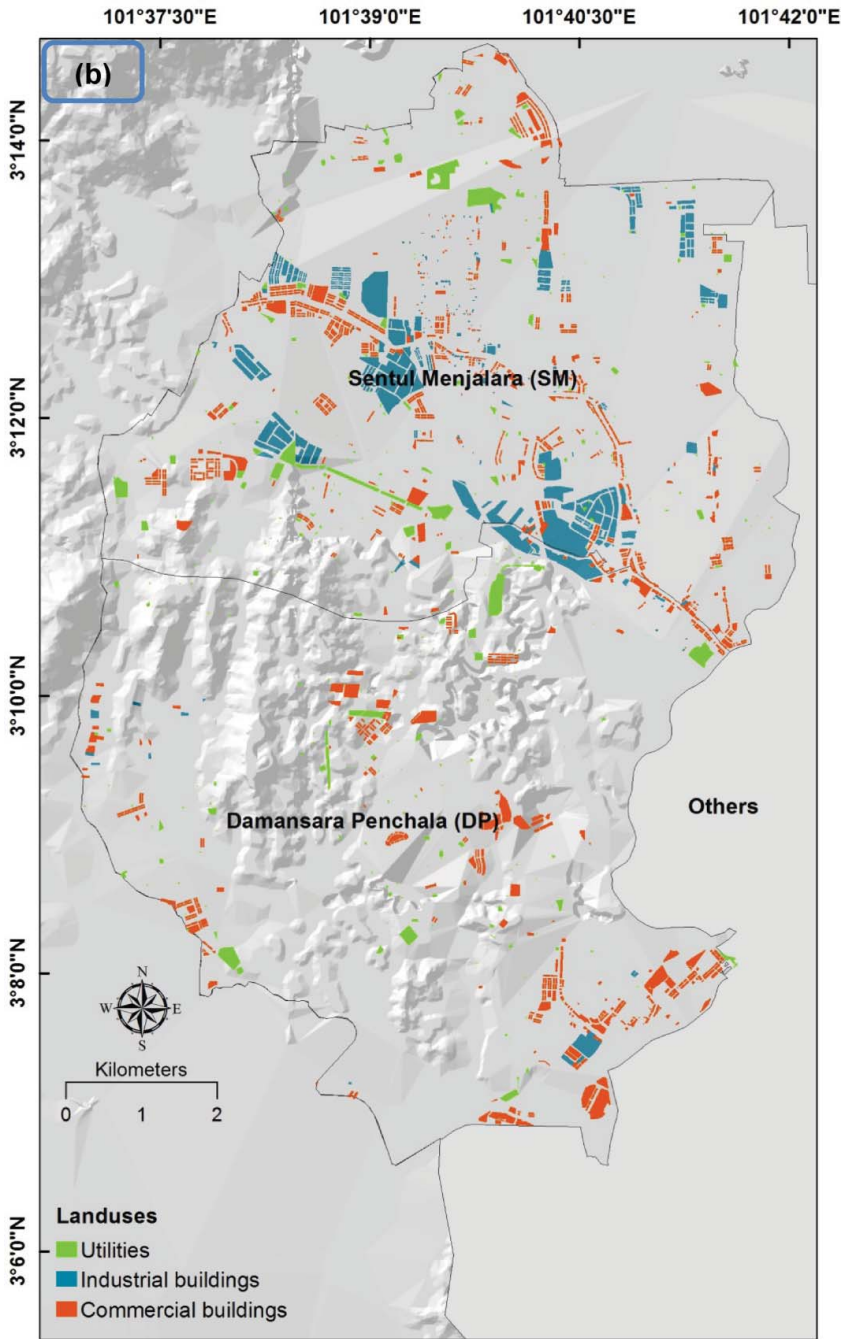


Figure 2. (Continued)

3.2. Method for landslide risk analysis

To conduct semi-quantitative risk analysis, a landslide hazard map was initially prepared. Hazard mapping results from the integrated relationship between temporal and spatial probabilities and magnitude (Guzzetti et al. 1999; Zêzere et al. 2004; Guzzetti et al. 2005). Given that this work is a

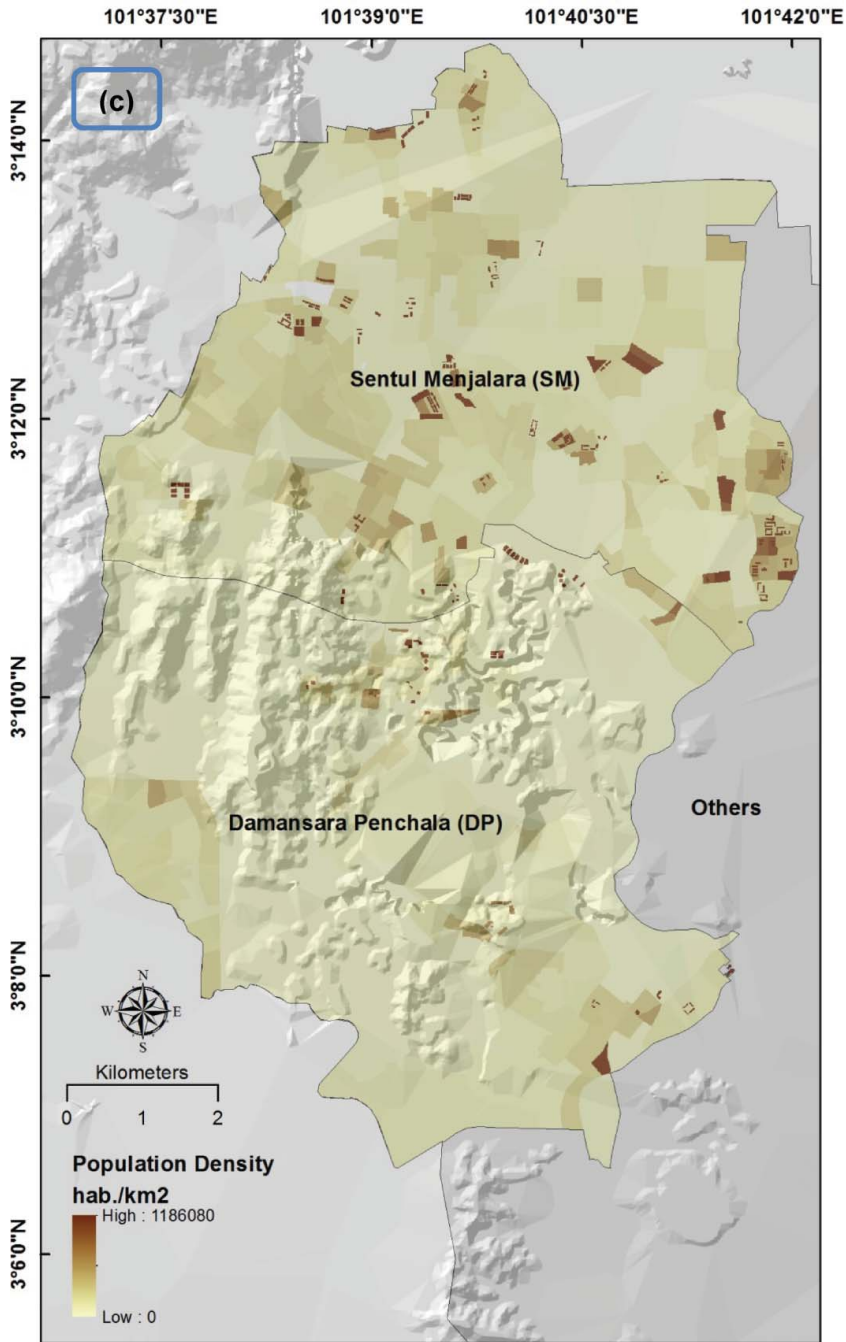


Figure 2. (Continued)

follow-up to Althuwaynee et al. (2015) (i.e. conducted by the same group of authors), the estimation of rainfall threshold and the landslide hazard map were obtained from the previous literature. Accordingly, details regarding the spatio-temporal hazard map are excluded from the current study and can be referred to in Althuwaynee et al. (2015).

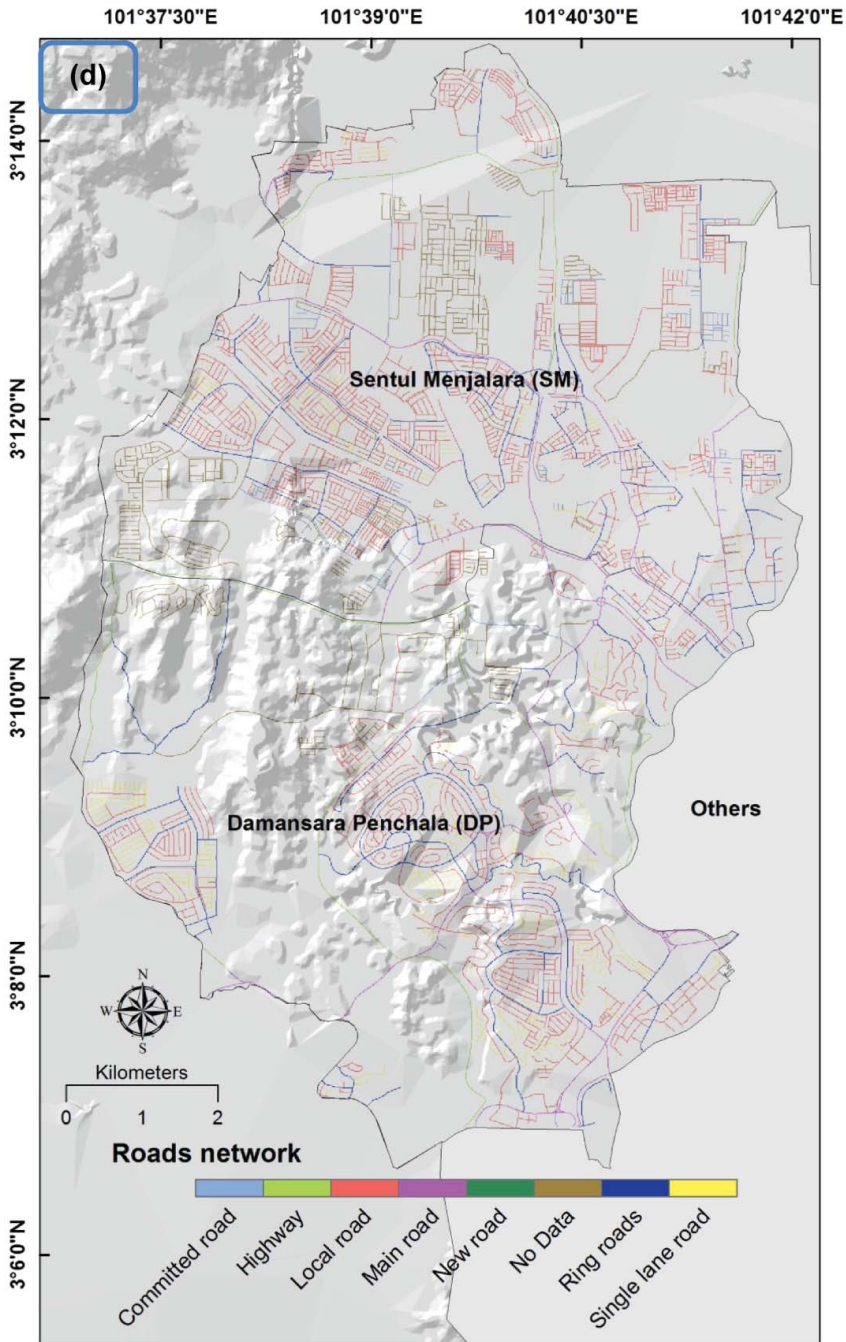


Figure 2. (Continued)

3.3. Landslide spatial probability (P_s)

Landslide P_s (spatial probability) refers to the likelihood of the occurrence of landslides given specific terrain conditions or to the spatial probability without considering the probability of occurrence of the triggering factors (Guzzetti et al. 2005; Fell et al. 2008). Training data were selected based on the nature of pattern distribution using the nearest-neighbour index (NNI) (Clark & Evans 1954) to

test the spatial nature pattern of landslide events and to measure and test randomness. The NNI method uses a ratio between two distances, i.e. the nearest-neighbour distance and the mean random nearest-neighbour distance chances (Althuwaynee & Pradhan 2014). The results showed that the percentages of clustered and dispersed were 85% and 15%, respectively, thereby indicating that landslides exhibited a cluster pattern tendency. Topographic factors were extracted from the digital elevation model using the survey contour points from 1:25,000 scale line and point coverage topographic maps. The lithology map was extracted from 1:63,300 scale polygon coverage geological maps. The normalized difference vegetation index (NDVI) was extracted from a Landsat TM image (Althuwaynee et al. 2012).

Fourteen landslide conditioning factors were used as input data layers in the analysis, namely slope, aspect, curvature, altitude, surface roughness, lithology, distance from faults, NDVI, land cover, distance from drainage, distance from road, stream power index, soil type, and precipitation. The spatial probability was determined using the statistical evidential belief function (EBF) model based on Dempster–Shafer theory of belief (Carranza & Hale 2003). The prediction results showed a promising area under the prediction curve value using the belief function map (Figure 3(a)) (Althuwaynee et al. 2012).

3.4. Landslide temporal probability

Intense and prolonged rainfalls triggered major landslides that cost lives and resulted in economic losses in the study area. In the present study, analysis was conducted after the completion of the rainfall-triggered landslide inventory from 2000 to 2012. Rainfall thresholds represented the main component of temporal probability (P_T), and thus, the daily antecedent relationship threshold was prepared using the daily rainfall of the registered landslide and four antecedent periods: 5-, 10-, 15-, and 30-day relationships; the relationship was also applied to the maximum non-landslide rainfall data, including the four antecedent periods (Guzzetti et al. 2005; Zezere et al. 2005; Tien Bui et al. 2013).

Daily rainfall data were collected from six automated tipping bucket rain gauges (Figure 3(b)) that were located in the centre of each study area. The gauges automatically recorded the amount, intensity, and duration of rainfall from 2000 to 2012, and data were provided by the Department of Irrigation and Drainage (DID), Malaysia. In the temporal prediction of landslides, previous landslide events were used and analysed to identify the periods of landslide reoccurrence (Althuwaynee et al. 2015). The temporal probability of a landslide initiation was calculated in the six zones at different periods. After calculating temporal probability, the frequency of excess daily rainfall was calculated for the next one, three, and five years using the records from 2000 to 2012. Further details regarding the hazard analysis procedure and results are found in Althuwaynee et al. (2015).

The empirical model of Poisson distribution (a continuous-time model) was used to estimate the relative frequency of landslide occurrence after the threshold was exceeded (Guzzetti et al. 1999; Crovelli 2000; Jaiswal et al. 2010; Tien Bui et al. 2013). In general, Poisson probability was applied to test both the exceedance probability of short mean recurrence intervals and time, which contribute mainly in determining the degree of hazards.

Reliability test was performed (Lee et al. 2014) to find the maximum value of reliability. Thresholds were produced based on the following relationship: $R_{\text{Threshold } 3,10,15,30} - A_{\text{Antecedent } 10,15,20,30}$. Subsequently, the major landslide threshold with a higher reliability index was selected (Althuwaynee et al. 2015).

3.5. Landslide hazard assessment

Some articles regarded the susceptibility map as the only component of a hazard map because of the scarcity of data (Chau et al. 2004). In the present study, landslide hazard assessment was achieved by multiplying the two main independent components (Equation (3)), namely (1) the spatial

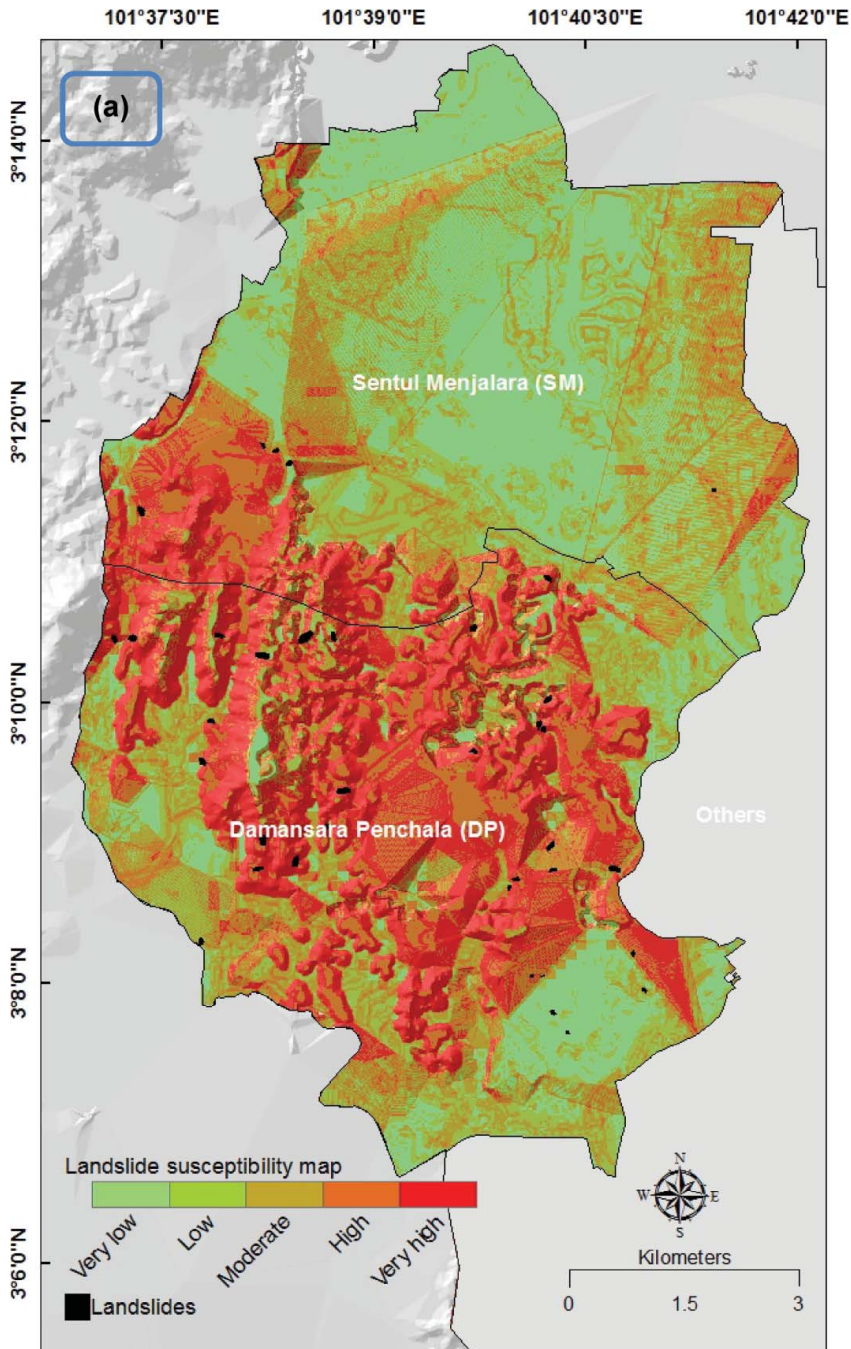


Figure 3. (a) Susceptibility map of KL city (adopted from Althuwaynee et al. 2015). (b) Hazard map of KL city with temporal and spatial integration (adopted from Althuwaynee et al.).

probability of the determinant or conditioning factors (or sliding conditions), and (2) the temporal probability of the occurrence of the triggering condition that results in a landslide (Guzzetti et al. 2005). The probability of exceeding a certain size, as discussed by Guzzetti (2005), was not included in the current research. P_s considers the comparison between the spatial distribution (dependent

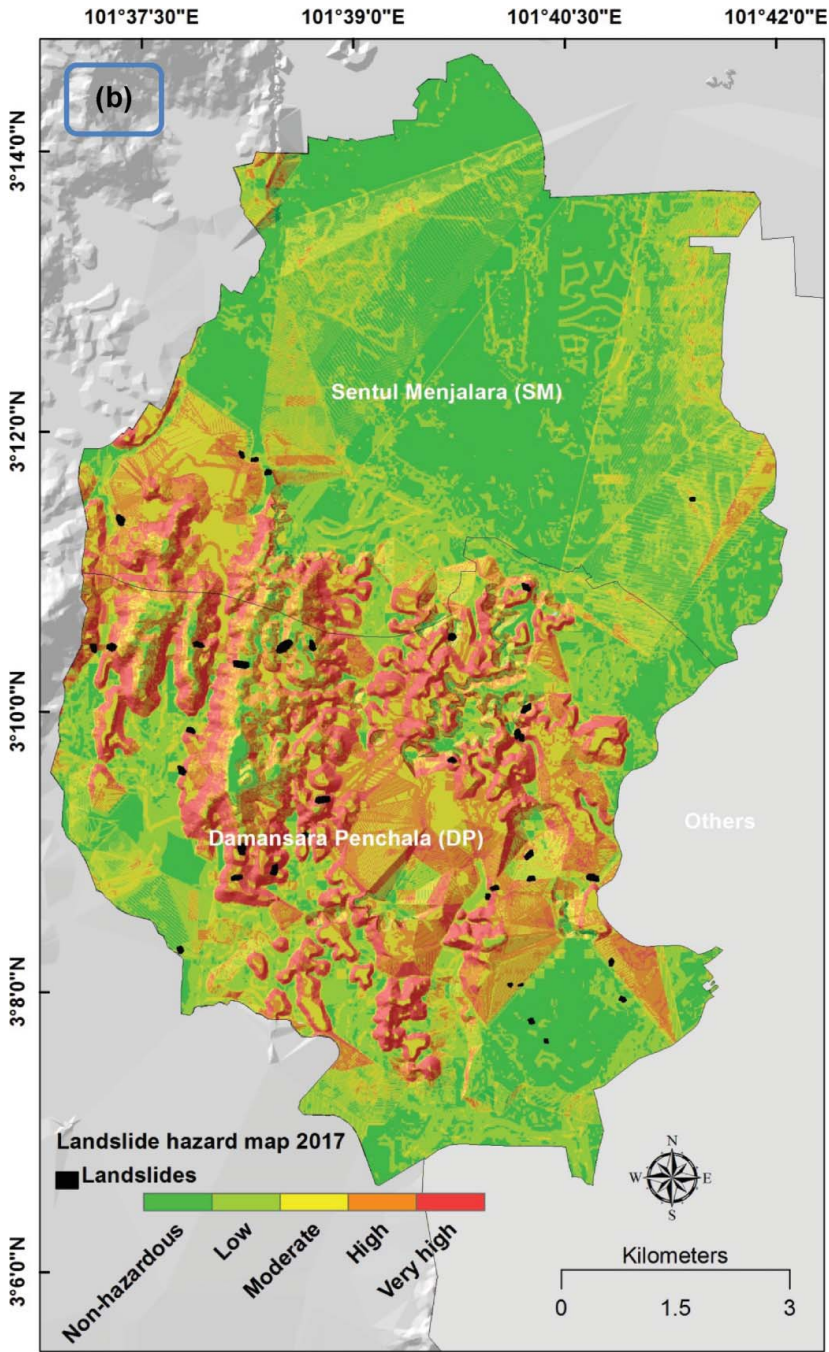


Figure 3. (Continued)

factor) of landslide inventory and landslide conditioning factors (independent factors). The results are likely to predict the conditions that may exist to produce future spatial instability. P_T is based on the theoretical assumption of the probability model, which provides the rainfall probability of occurrence (R) that exceeds the threshold limit (R_T). The equation states that landslide (L) probability is equal to the probability of the exceeded rainfall ($R > R_T$) multiplied by the probability of the

occurrence of a landslide (Jaiswal et al. 2010):

$$\text{Hazard } (H) = P_S \times P_T \quad (3)$$

The hazard map was classified into five natural break zones (Irigaray et al. 2007): not hazardous, low, moderate, high, and very high (Figure 3(b)). The details regarding the hazard map is available in Althuwaynee et al. (2015).

3.6. Landslide risk assessment

The hazard map was used to detect the exposure of landslide at elements under risks per mapping unit (e.g. multi-themes of land uses). To estimate risks according to land use and population density, an exposure-based approach applied in rock-fall hazards (Lee & Jones 2004) and in medium-scale, deep-seated, and shallow landslides (Ghosh et al. 2012) was adopted in the current analysis.

High-resolution land-use data were used to find the actual distribution of buildings within each SU. In the current analysis, no detailed report was used regarding actual damages that might occur after landslide events. Therefore, the current procedure aimed to extract and indicate the prone elements in each SU. In the case of road networks, classification based on available data was considered, including committed roads, new roads, local roads, single-lane roads, ring roads, main roads, and highways. Unit length was used instead of number of losses. In particular, the following steps were performed in the assessment:

- (1) A fishnet grid with a cell dimension of 250 m \times 250 m (i.e. an SU) was created using the data management tools of ArcGIS software (Chandel et al. 2011; Samadi et al. 2014). For easy interpretation, the current fishnet cell size must be between that of a medium-scale hazard map and the scale of a land-use density map.
- (2) The number of objects (i.e. buildings in residential areas) per SU was calculated.
- (3) The hazard map was classified into five natural break zones (Irigaray et al. 2007; Constantin et al. 2011) (from not hazardous to highly hazardous), which were then converted into polygons. The clip and union tools under spatial management tools were used to extract each footprint of the land-use elements from the hazard layer.
- (4) The number of affected elements in each SU (L_{SU}) was calculated as follows:

$$L_{SU} = \text{Cell}_{\text{aff } SU} \times P_{\text{Cell}_{\text{occ}}} \quad (4)$$

where $\text{Cell}_{\text{aff } SU}$ is the number of elements of a given class in an SU that contribute to the hazard value (0 to 1), and $P_{\text{Cell}_{\text{occ}}}$ is the probability of cells being occupied by an element at risk.

- (5) The vulnerability value and the initial cost of the construction for the element at risk were assumed to be 1 because of data scarcity. Thus, the hazard value was regarded only as a guide to determine the number of losses (Figure 4).
- (6) Finally, the final risk map was produced by assigning the results of Equation (4) to each element (Armaş 2014).

4. Results and discussion

The few gaps identified by the current study must be addressed in future works given that they measure the uncertainty of the current results and the limitation of the study scope. The magnitude-frequency analysis plays a vital role in vulnerability index production (e.g. inverse gamma). Therefore, a complete data-set that includes landslide size (large- and medium-scale slope failures) and types of mass movements (shallow and rapid landslides and slow and deep-seated landslides) can

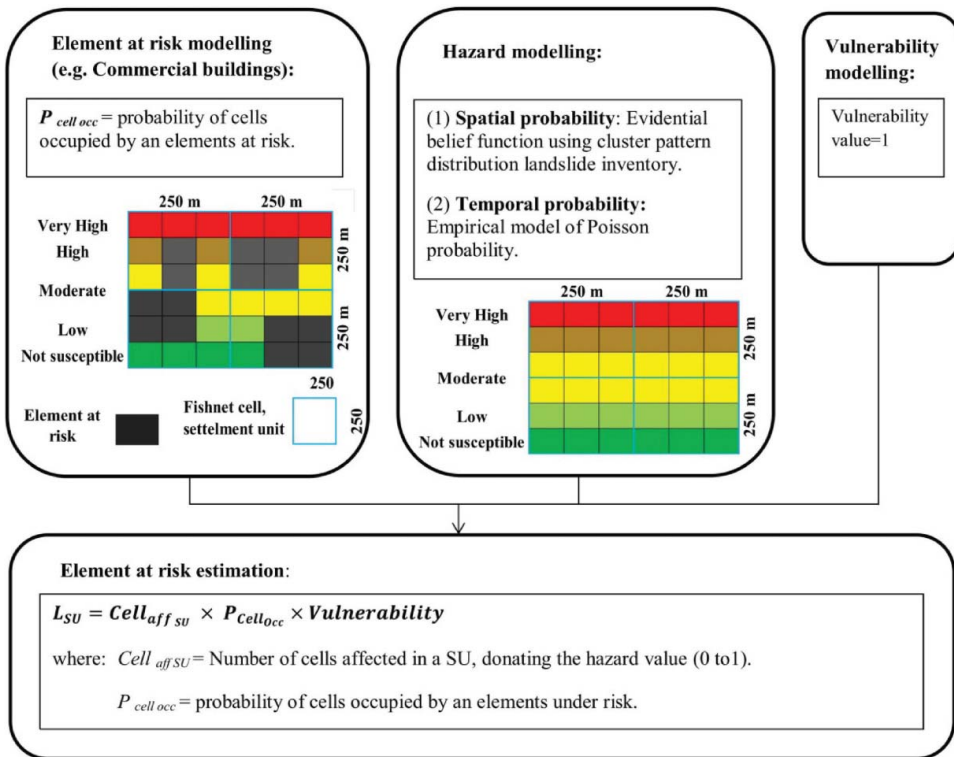


Figure 4. Methodology adopted for calculation of building losses estimation.

enhance landslide risk assessment. Incomplete damage records make validating the current findings difficult (Ghosh et al. 2011).

For brevity, details regarding the hazard analysis process and related figures and validation results were not included in this paper. Instead, the landslide hazard map and supportive results are found in Althuwaynee et al. (2015). The exposure map shows the elements at risk exposed to different levels of landslide hazards compared with their vulnerability to expected damages. The complex procedure of data acquisition and database generation is extremely critical in developing countries such as Malaysia because no single nominated agency maintains a complete landslide database. Given these limitations, we simplified the vulnerability value to 1 (total losses) for all land-use components in each SU and changed the expected results to the number of affected elements instead of the degree of losses (e.g. number of injured or fatalities for population and initial or partial collapse for buildings) (Erener & Düzgün 2013). Therefore, the current study tested the use of medium-scale (1:25,000) hazard map data in semi-quantitative landslide risk assessment and focused mainly on the investigation of expected losses of elements at risk because of the aforementioned data constraints.

4.1. Expected damage risk to land use and population

From the sequence of affected elements at risk, a major percentage of affected elements are related to utilities, residential, and commercial, followed by population and industrial elements. Nearly half to two-thirds of the total area of industrial buildings zones are categorized as not hazardous (which indicates an appropriate selection of the industrial site beyond the landslide-prone areas). Meanwhile, 12% of utilities elements fall within the very highly hazardous region. Although such

Table 3. Amount of land-use elements and population density likely to be affected for different landslide hazard classes.

Type	Total amount	Total amount of units in hazardous areas:					Total losses	Total losses percentage
		Non-hazardous	Low	Moderate	High	Very high		
Residential	43,602 elements	13,785 (32%)	12,800 (29%)	8803 (20%)	5787 (13%)	2427 (6%)	21,913	50%
Commercial	6600 elements	3034 (46%)	2001 (30%)	811 (12%)	502 (8%)	252 (4%)	2340	35%
Industrial	1991 elements	937 (47%)	824 (41%)	201 (10%)	25 (1%)	4 (0%)	617	31%
Utilities	1,226,700 area (m ²)	300,600 (25%)	386,600 (32%)	212,100 (17%)	174,100 (14%)	153,300 (12%)	382,328	31%
Population	493,963 (hab./107 km ²)	79,964 (hab./107 km ²) (52%)	42,849 (hab./107 km ²) (27%)	11,313 (hab./107 km ²) (14%)	8190 (hab./107 km ²) (4%)	4955 (hab./107 km ²) (3%)	147,270 (hab./107 km ²)	18%

percentage appears to be low, it remains significant given the limited number of utilities in the entire study area. Consequently, 12% is the largest percentage among the remaining land uses, which indicates incidental site selection for the aforementioned important land-use components.

Land use that falls under the very high hazard class requires close attention from the government, which must take appropriate actions to address future landslide threats. Population densities represent the number of people linked to their houses as a static representation (the number of people during the day was excluded from the analysis). Approximately 15% of the population resides in common hazardous areas (moderate to very high hazard). [Table 3](#) presents the number of buildings classified based on land-use categories, and [Figure 5](#) shows the percentages of expected affected elements.

[Figure 6\(a\)](#) shows the expected range of residential buildings that can be affected by different classes of hazard events. The density of buildings can positively and negatively affect the variation of elements. The western and southern areas of Damansara Penchala, particularly in certain areas, such as Taman Tun Dr. Ismail and Bangsar Baru, are active landslide-threat areas. Thus, approximately 100–250 units per SU are located in very high-risk areas. The western part of Sentul Menjalara, represented by Taman Bukit Maluri, has experienced repeated landslide scenarios. This condition can increase the risk index in the area to 270 units per SU.

[Figure 6\(b\)](#) shows the range of commercial buildings that can be directly affected by hazard events. The expected number of building loss ranges from 45 to 66 units in each SU in the central part of the Damansara Penchala zone and in the western part of the Sentul Menjalara zone. The highest density of commercial buildings is located in the south-eastern and central areas of Damansara Penchala and Sentul Menjalara; the expected losses in these areas are less than 20 units. [Figure 6\(c\)](#) shows the range of industrial buildings in high- to low-risk hazardous areas. A major percentage of industrial buildings (90%) are located in the centre of the Sentul Menjalara zone. The centre of Sentul Menjalara is considered the safest zone, but its western part is characterized by high building density; thus, expected losses in that area reach approximately 45 units in some SUs. Similarly, [Figure 6\(d\)](#) shows the range of utilities that mainly consists of electrical establishments and sewage systems. In this case, the unit of area was used to describe losses instead of the number of buildings. The components of multiple utilities are located in the border of two zones. These components are generally considered safe because they are uniformly distributed on areas with low to medium hazard.

High population density has a direct relationship with the high density of residential buildings ([Figure 6\(e\)](#)). The Sentul Menjalara zone has a higher density compared with the Damansara Penchala zone and faces serious landslide threats, particularly in the western part where the population density is between 700 and 1500 persons/acre.

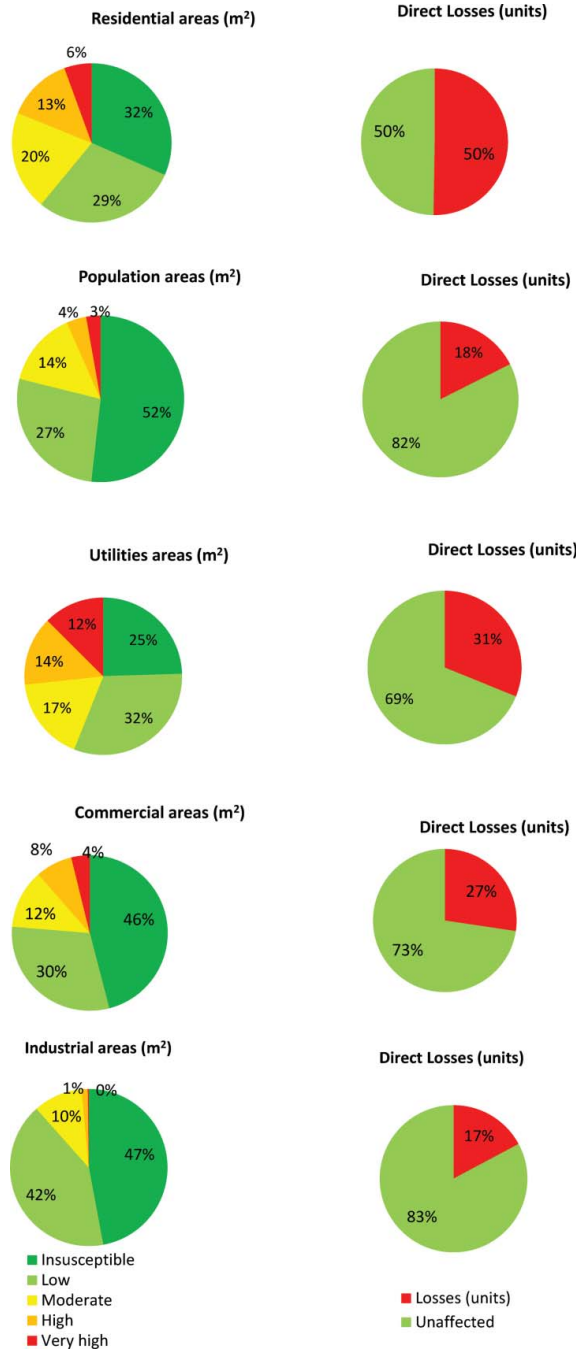


Figure 5. Percentages of land-use units and population density likely to be affected for different landslide hazard classes.

The results did not include the relationship between people living inside buildings and landslide events. Instead, each component was considered in a separate analysis because data on land use and population were provided by two agencies that followed different allocation and acquisition procedures.

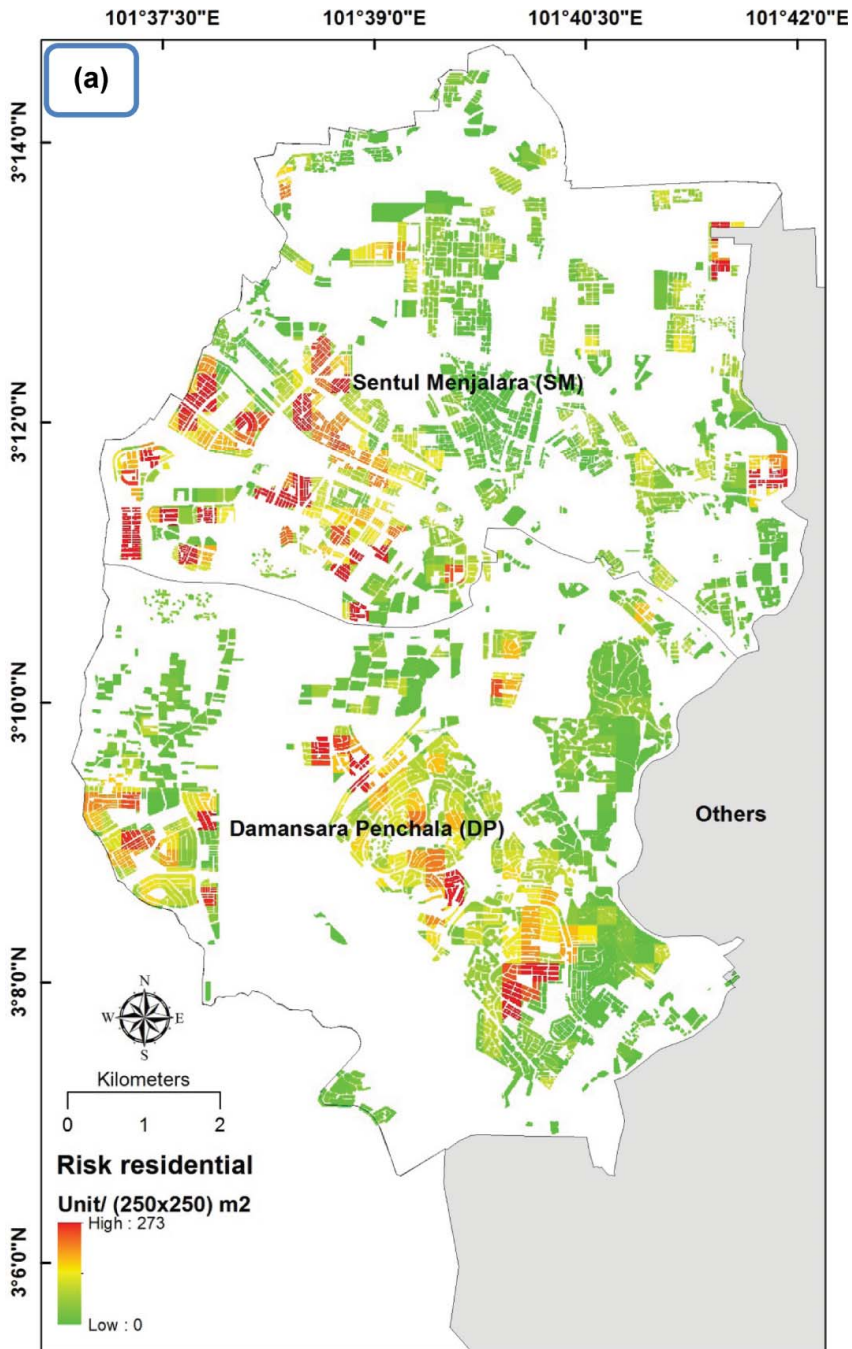


Figure 6. Risk map showing spatial distribution of likely losses of (a) affected residential buildings; (b) affected commercial buildings; (c) affected industrial buildings; (d) affected utilities areas; (e) affected population density; and (f) affected roads network.

4.2. Expected damage risk to road networks

Seven categories of road data (i.e. committed roads, new roads, local roads, single-lane roads, ring roads, main roads, and highways) were derived to identify the relationship of road networks with landslide hazard classes. Table 4 presents the total amount of roads measured by unit length.

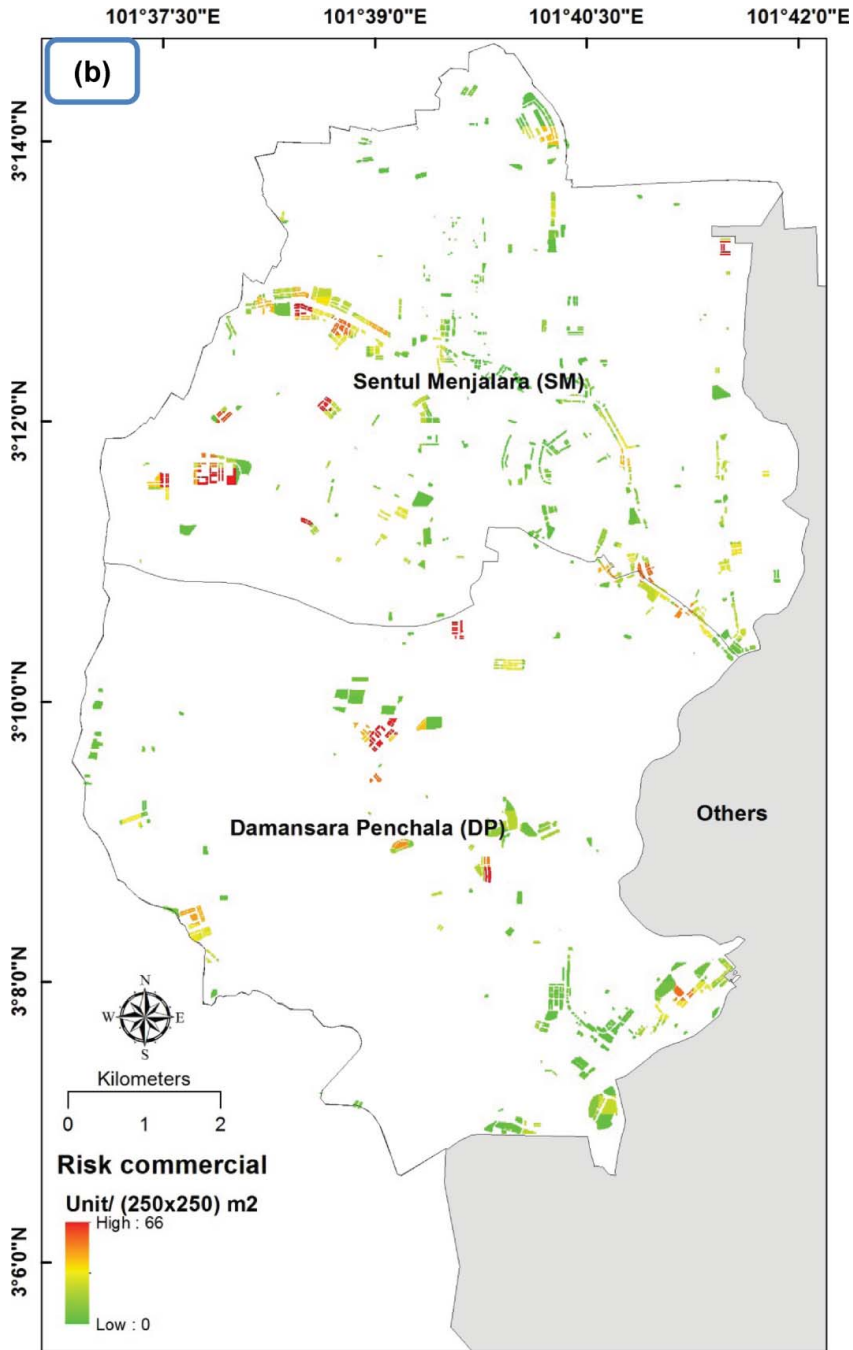


Figure 6. (Continued)

Highways can have the highest percentage of losses, followed by main roads, committed roads, and ring roads. A high percentage of highways with considerable road lengths are located in very highly hazardous areas. By contrast, nearly 70% of main roads are located in non-hazardous areas. Other road types have inconsistent ratios that fall under non-hazardous, low, and moderate areas.

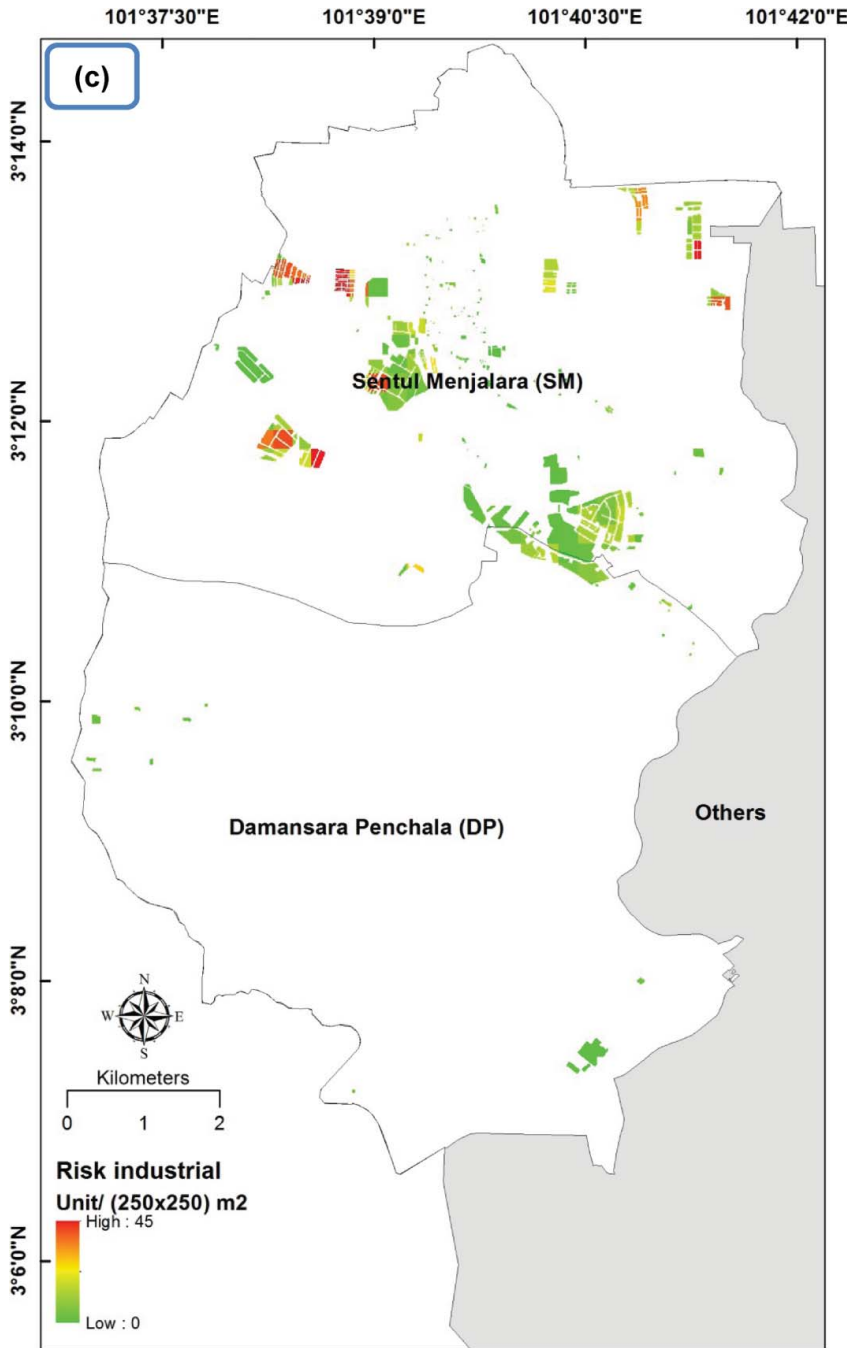


Figure 6. (Continued)

Figure 6(f) shows the expected losses in road networks determined by applying the exposure-based method of loss estimation. Significant losses can be observed along highways with a length of over 10 km because most highways pass through the highly hazardous areas in the northern, western, and southern Damansara Penchala zones. The constant loss value is nearly 25% for local roads,

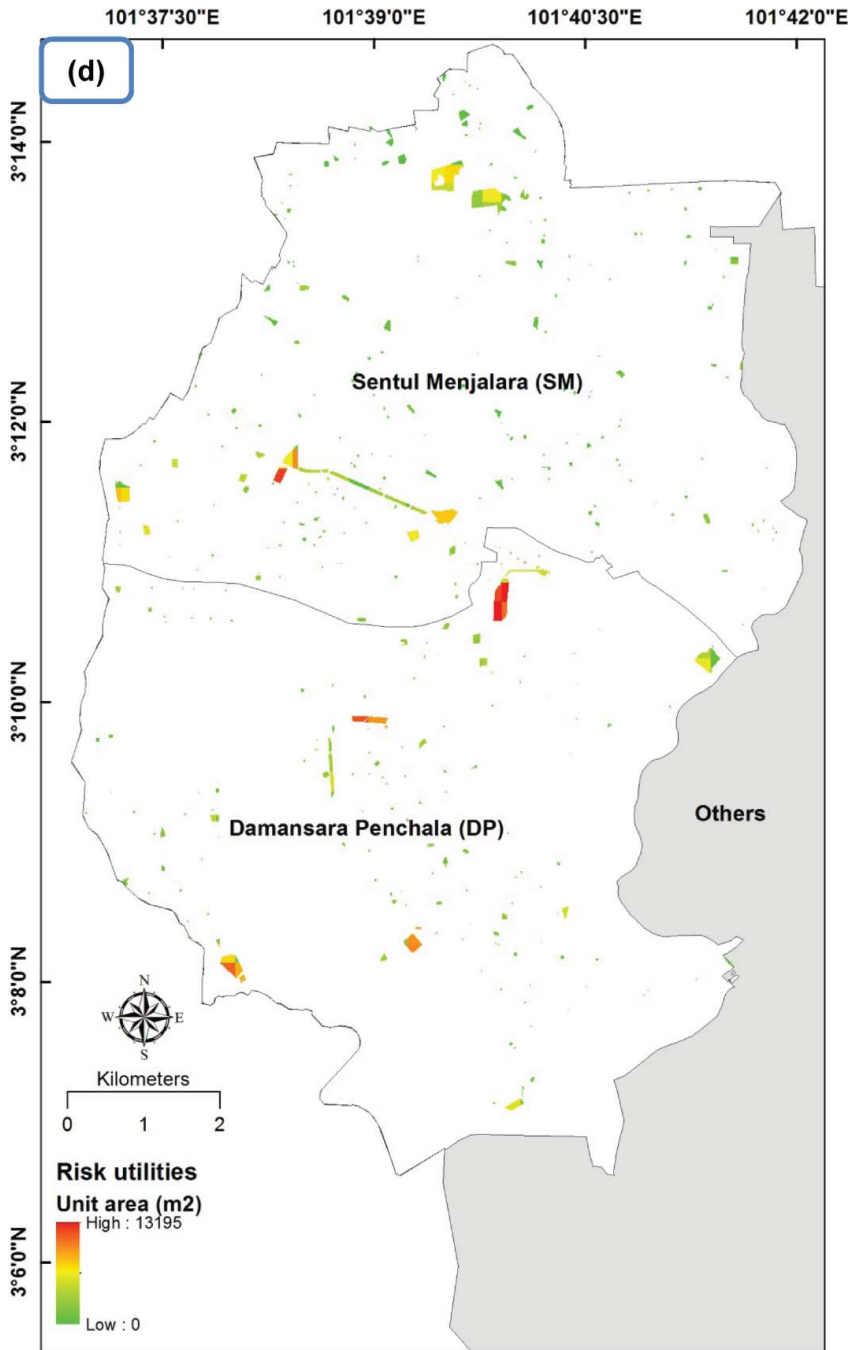


Figure 6. (Continued)

single-lane roads, and ring roads. Jalan Mahameru, which is considered one of the main roads in the south-eastern part of the Damansara Penchala zone, experienced a landslide event on 14 January 2014. The debris caused kilometres of massive traffic jams. A total of 120 km of roads fall within landslide-prone areas, and thus, are expected to suffer from multiple landslide events in the future. Accordingly, extensive monitoring plans are required.

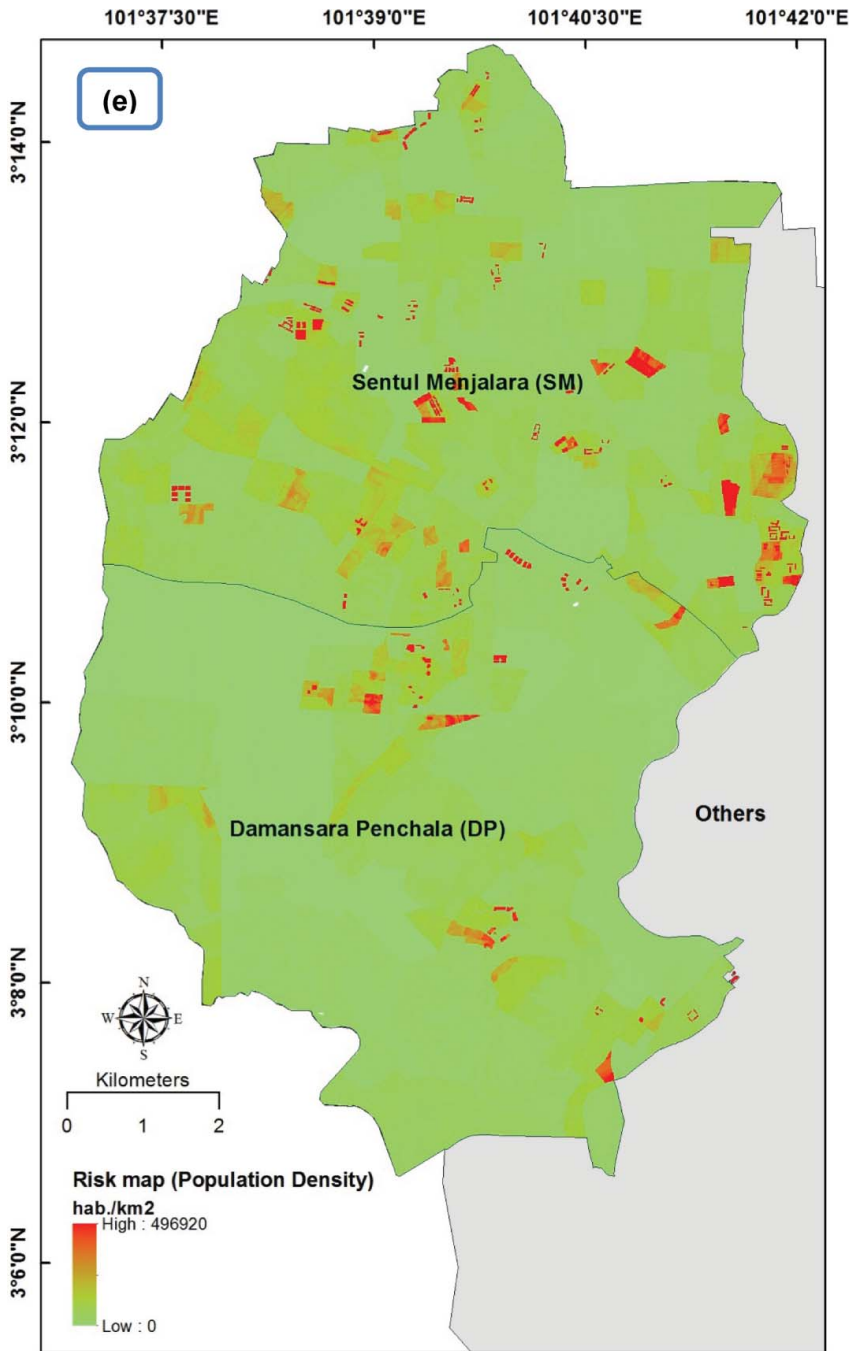


Figure 6. (Continued)

The aforementioned results indicated that the percentages of affected elements were approximately 50% in residential areas, 35% in commercial buildings, 31% in industrial buildings, and 31% in utility areas. The percentages of affected elements in population and road network were approximately 18% and 27%, respectively.

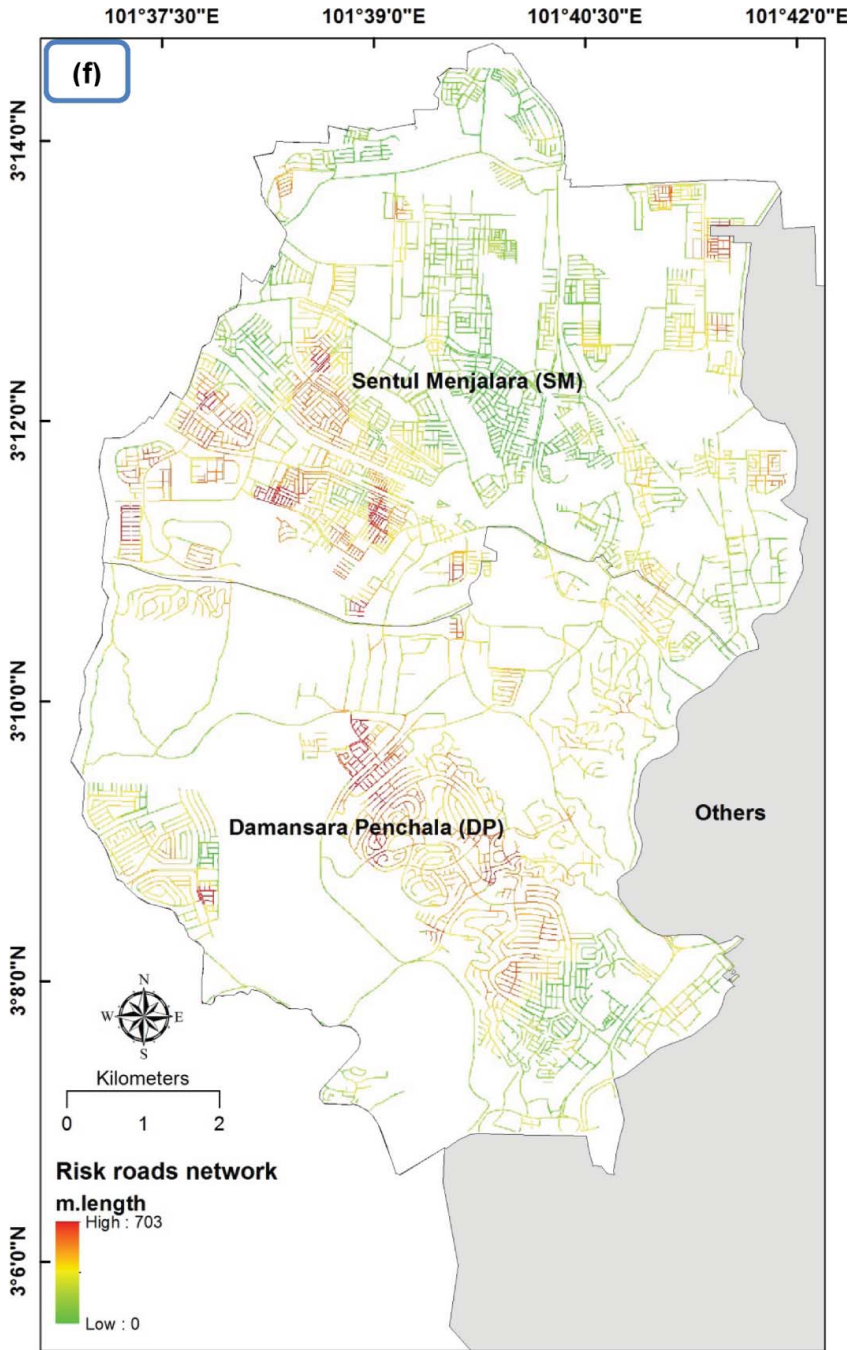


Figure 6. (Continued)

Guikema (2009) presented specific assumptions that should be followed to enhance theory of construction design in hazardous areas, such as (1) enhancing the design stage (e.g. cost–benefit relationship in different design alternatives), (2) determining the level of robustness of a design (e.g. contaminant releases, degradation of ecosystems), and (3) considering natural modes of ecosystem protection (e.g. design of a levee).

Table 4. Total amount of roads unit length likely to be affected for different landslide hazard classes.

Roads type	Total length	Total amount of units in hazardous areas (km)										Total losses	Losses percentage
		Non-hazardous		Low		Moderate		High		Very high			
No data	134	35	26%	31	23%	24	18%	26	20%	15	11%	41	31%
Committed roads, no data	29	7	25%	10	36%	6	21%	3	11%	2	7%	8	28%
New roads	0.17	0.11	66%	0	18%	0	5%	0	5%	0	6%	0.01	5%
Local roads	347	115	34%	107	32%	63	19%	39	11%	15	5%	85	25%
Single-lane roads	59	18	31%	16	29%	12	20%	8	14%	2	6%	15	25%
Ring roads	106	29	28%	31	30%	21	20%	17	16%	6	6%	29	27%
Main road	51	13	26%	19	38%	8	16%	7	14%	3	6%	14	28%
Highways	32	8	24%	9	28%	5	16%	5	15%	5	15%	10	32%
Total roads network	759											203	27%

5. Conclusion

The current study attempts to contribute to the development of a semi-quantitative approach for landslide risk assessment despite insufficient data-set on the historical inventory and physical building assessment of Kuala Lumpur. Moreover, an overview on potential building damages, as well as the safety factor of different structure types (single- and double-storey houses or apartments), is not available. In this highly scarce data environment, the semi-quantitative analytical model adopted in this study was able to predict possible losses of elements at risk (i.e. exact number of affected people rather than the actual number of expected injuries or fatalities). This study extended the previous landslide hazard assessment. First, a susceptibility map (spatial probabilities) was completed using the statistical EBF method. Afterwards, Poisson probability was applied to test both the exceedance probability of short mean recurrence intervals and time (Althuwaynee et al. 2015). The vulnerability value was simplified and generalized for all land-use components in each SU.

The result of risk was determined for specific elements at risk in the land use, population density, and road network maps. Land-use elements located in the centre of Sentul Menjalara are the safest compared with those in the western and southern parts. For the population density map, although the Damansara Pencil zone suffers from frequent historical landslides, it is considered less hazardous than the southern Sentul Menjalara zone, i.e. the second most densely populated area falling within hazardous zones. Meanwhile, the highest percentages of affected elements were found in residential areas, commercial buildings, industrial buildings, utility areas, and highly populated areas. Moreover, high to low percentages of losses for road networks were found in highways, main roads, committed roads, and ring roads. The results of the semi-quantitative risk assessment provide unique and essential information on landslide-prone areas with up-to-date multi-themed land-use maps.

Finally, the few gaps identified by the current study must be addressed in future works given that they measure the uncertainty of the current results and the limitation of the study scope. A magnitude–frequency analysis plays a vital role in vulnerability index production (e.g. inverse gamma). Therefore, a complete data-set that includes landslide size (large- and medium-scale slope failures) and types of mass movements (shallow and rapid landslides and slow and deep-seated landslides) can contribute to enhancing landslide risk assessment. However, incomplete damage records make validating the current findings a challenging task (Ghosh et al. 2011).

Acknowledgments

The authors acknowledge and appreciate the provision of rainfall and landslide data by the Department of Irrigation and Drainage DID, Malaysia. Also, we would like to appreciate the provision of land uses, population density, and roads network data by Jabatan Perangkaan, Malaysia, or Department of Statistics, Malaysia, and Dewan Bandaraya Kuala Lumpur or Kuala Lumpur City Hall DBKL. Also, the authors gratefully acknowledge the financial support from the UPM-RUGS project grant, vote number: 9344100.


Disclosure statement


No potential conflict of interest was reported by the authors.

Funding

Faculty of Engineering, University Putra Malaysia UPM-RUGS project grant (vote number: 9344100)

ORCID

Omar F. Althuwaynee  <http://orcid.org/0000-0001-9863-2046>

Biswajeet Pradhan  <http://orcid.org/0000-0001-9863-2054>

References

- Althuwaynee O, Pradhan B. 2014. An alternative technique for landslide inventory modeling based on spatial pattern characterization. In: Abdul Rahman A, Boguslawski P, Anton F, Said MN, Omar KM, editors. *Geoinformation for informed decisions*. Switzerland: Springer International Publishing; p. 35–48.
- Althuwaynee OF, Pradhan B, Ahmad N. 2015. Estimation of rainfall threshold and its use in landslide hazard mapping of Kuala Lumpur metropolitan and surrounding areas. *Landslides*. 12:861–875.
- Althuwaynee OF, Pradhan B, Lee S. 2012. Application of an evidential belief function model in landslide susceptibility mapping. *Comp Geosci*. 44:120–135.
- Armaş I. 2014. Diagnosis of landslide risk for individual buildings: insights from Prahova Subcarpathians, Romania. *Environ Earth Sci*. 71:4637–4646.
- Bell R, Glade T. 2004. Quantitative risk analysis for landslides – examples from Bildudalur, Nw-Iceland. *Nat Hazards Earth System Sci*. 4:117–131.
- Carranza EJM, Hale M. 2003. Evidential belief functions for data-driven geologically constrained mapping of gold potential, Baguio District, Philippines. *Ore Geol Rev*. 22:117–132.
- Carrara A, Crosta G, Frattini P. 2003. Geomorphological and historical data in assessing landslide hazard. *Earth Surf Proc Landforms*. 28:1125–1142.
- Catani F, Casagli N, Ermini L, Righini G, Menduni G. 2005. Landslide hazard and risk mapping at catchment scale in the Arno River basin. *Landslides*. 2:329–342.
- Chandel VB, Brar KK, Chauhan Y. (2011) Rs & gis based landslide hazard zonation of mountainous terrains. A study from middle Himalayan Kullu District, Himachal Pradesh, India. *Int J Geomatics Geosci*. 2:121–132.
- Chau K, Sze Y, Fung M, Wong W, Fong E, Chan L. 2004. Landslide hazard analysis for Hong Kong using landslide inventory and GIS. *Comp Geosci*. 30:429–443.
- Clark PJ, Evans FC. 1954. Distance to nearest neighbor as a measure of spatial relationships in populations. *Ecology*. 35:445–453.
- Constantin M, Bednarik M, Jurchescu MC, Vlaicu M. 2011. Landslide susceptibility assessment using the bivariate statistical analysis and the index of entropy in the Sibiciu basin (Romania). *Environ Earth Sci* 63:397–406.
- Corominas J, Moya J. 2008. A review of assessing landslide frequency for hazard zoning purposes. *Eng Geol* 102:193–213.
- Crovelli RA. 2000. Probability models for estimation of number and costs of landslides. US Geological Survey. (Open file Report 00-249). Available from <http://pubs.usgs.gov/of/2000/ofr-00-0249/ProbModels.html>,
- Crozier MJ, Glade T. 2006. *Landslide hazard and risk: Issues, concepts and approach*. West Sussex: Wiley; p. 1–40.
- Das IC. 2011. *Spatial statistical modelling for assessing landslide hazard and vulnerability*. Enschede: University of Twente.
- de Noronha Vaz E, Caetano M, Nijkamp P. 2011. A multi-level spatial urban pressure analysis of the Giza pyramid plateau in Egypt. *J Herit Tour*. 6:99–108.
- Erener A, Düzgün HS. 2013. A regional scale quantitative risk assessment for landslides: case of Kumluca watershed in Bartın, Turkey. *Landslides*. 10:55–73.
- Fell R. 1994. Landslide risk assessment and acceptable risk. *Can Geotech J*. 31:261–272.
- Fell R, Corominas J, Bonnard C, Cascini L, Leroi E, Savage WZ. 2008. Guidelines for landslide susceptibility, hazard and risk zoning for land use planning. *Eng Geol*. 102:99–111.
- Ghosh S, Carranza EJM, van Westen CJ, Jetten VG, Bhattacharya DN. 2011. Selecting and weighting spatial predictors for empirical modeling of landslide susceptibility in the Darjeeling Himalayas (India). *Geomorphology*. 131:35–56.
- Ghosh S, van Westen CJ, Carranza EJM, Jetten VG. 2012. Integrating spatial, temporal, and magnitude probabilities for medium-scale landslide risk analysis in Darjeeling Himalayas, India. *Landslides*. 9:371–384.

- Glade T. 2003. Landslide occurrence as a response to land use change: a review of evidence from New Zealand. *Catena*. 51:297–314.
- Glade T, Anderson M, Crozier MJ. 2005. *Landslide hazard and risk*. Chichester: John Wiley & Sons Ltd.
- Guikema SD. 2009. Infrastructure design issues in disaster-prone regions. *Science*. 323:1302–1303.
- Guzzetti F, Carrara A, Cardinali M, Reichenbach P. 1999. Landslide hazard evaluation: a review of current techniques and their application in a multi-scale study, central Italy. *Geomorphology*. 31:181–216.
- Guzzetti F, Reichenbach P, Cardinali M, Galli M, Ardizzone F. 2005. Probabilistic landslide hazard assessment at the basin scale. *Geomorphology*. 72:272–299.
- Hutchison CS. 1975. Ophiolite in Southeast Asia. *Geol Soc Am Bull*. 86:797–806.
- Irigaray C, Fernández T, El Hamdouni R, Chacón J. 2007. Evaluation and validation of landslide-susceptibility maps obtained by a GIS matrix method: Examples from the betic cordillera (southern Spain). *Nat Hazards*. 41:61–79.
- Jaiswal P, van Westen CJ, Jetten V. 2010. Quantitative landslide hazard assessment along a transportation corridor in southern India. *Eng Geol*. 116:236–250.
- Jaiswal P, van Westen CJ, Jetten V. 2011. Quantitative estimation of landslide risk from rapid debris slides on natural slopes in the Nilgiri Hills, India. *Nat Hazards Earth Syst Sci* 11.
- Jamaludin S, Hussein AN. 1993. *Landslide hazard and risk assessment: the Malaysian experience*. Notes.
- Lee E, Jones D. 2004. *Landslide risk assessment*. Thomas Telford. Westminster: ICE Publishing; p. 454.
- Lee ML, Ng KY, Huang YF, Li WC. 2014. Rainfall-induced landslides in Hulu Kelang area, Malaysia. *Nat Hazards*. 70:353–375.
- Lee S. 2007. Comparison of landslide susceptibility maps generated through multiple logistic regression for three test areas in Korea. *Earth Surf Proc Landforms*. 32:2133–2148. doi:10.1002/esp.1517
- Lee S, Pradhan B. 2007. Landslide hazard mapping at Selangor, Malaysia using frequency ratio and logistic regression models. *Landslides*. 4:33–41. doi:10.1007/s10346-006-0047-y
- Li Z, Nadim F, Huang H, Uzielli M, Lacasse S. (2010) Quantitative vulnerability estimation for scenario-based landslide hazards. *Landslides*. 7:125–134.
- Lu P, Catani F, Tofani V, Casagli N. 2014. Quantitative hazard and risk assessment for slow-moving landslides from persistent scatterer interferometry. *Landslides*. 11:685–696.
- McInnes R. 2007. *Landslides and climate change: challenges and solution*. Boca Raton (FL): CRS Press, Taylor & Francis Group.
- Nicolet P, Foresti L, Caspar O, Jaboyedoff M. 2013. Shallow landslides stochastic risk modelling based on the precipitation event of august 2005 in Switzerland: results and implications. *Nat Hazards Earth Syst Sci*. 13:3169–3184.
- Pazzi V, Morelli S, Fidolini F, Krymi E, Casagli N, Fanti R. 2016. Testing cost-effective methodologies for flood and seismic vulnerability assessment in communities of developing countries (Dajç, Northern Albania). *Geomatics Nat Hazards Risk*. 7:971–999.
- Promper C, Gassner C, Glade T. 2015. Spatiotemporal patterns of landslide exposure—a step within future landslide risk analysis on a regional scale applied in Waidhofen/Ybbs Austria. *Int J Disaster Risk Reduct*. 12:25–33.
- Quinn P, Hutchinson D, Diederichs M and Rowe R (2011) Characteristics of large landslides in sensitive clay in relation to susceptibility, hazard, and risk. *Can Geotech J*. 48:1212–1232.
- Remondo J, Bonachea J, Cendrero A. 2008. Quantitative landslide risk assessment and mapping on the basis of recent occurrences. *Geomorphology*. 94:496–507.
- Roberds W. 2005. *Estimating temporal and spatial variability and vulnerability*. London: Taylor and Francis; p. 129–157.
- Samadi HR, Teymoorian A, Ghasemi M. 2014. Landslide analysis to estimate probability occurrence of earthquakes by software ArcGIS in central of Iran. *Res J Recent Sci*. 3:104–109.
- Sassa K, Canuti P. 2008. *Landslides: disaster risk reduction*. Germany: Springer Verlag, Berlin Heidelberg.
- Schlögel R, Torgoev I, De Marneffe C, Havenith H-B. 2011. Evidence of a changing size–frequency distribution of landslides in the Kyrgyz Tien Shan, Central Asia. *Earth Surf Proc Landforms*. 36:1658–1669. doi:10.1002/esp.2184
- Schuster R. (1996) The 25 most catastrophic landslides of the 20th century. In: Chacon J, Irigaray C, Fernandez T, editors. *Landslides. Proceedings of the 8th International Conference and Field Trip on Landslides*. Rotterdam: Balkema; p. 1–18.
- Sidle RC, Ochiai H. 2006. *Landslides: processes, prediction, and land use*. Washington (DC): American Geophysical Union.
- Tien Bui D, Pradhan B, Lofman O, Revhaug I, Dick Ø B. 2013. Regional prediction of landslide hazard using probability analysis of intense rainfall in the Hoa Binh Province, Vietnam. *Nat Hazards*. 66:707–730.
- Trigila A, Spizzichino D, Iadanza C. 2010. The impact of landslides on urban areas and infrastructure in Italy. EGU General Assembly Conference Abstracts. p. 3286
- van Westen CJ, van Asch TWJ, Soeters R. 2006. Landslide hazard and risk zonation – why is it still so difficult? *Bull Eng Geol Environ*. 65:167–184. doi:10.1007/s10064-005-0023-0
- Varnes DJ, The International Association of Engineering Geology Commission on Landslides and Other Mass Movements on Slopes. 1984. *Landslide hazard zonation: a review of principles and practice*. Vol. 3, Natural hazards. Paris: United Nations Educational, Scientific and Cultural Organization; p. 63.
- Varnes DJ. 1984. *Landslide hazard zonation – a review of principles and practice*. Paris: IAEG Commission on Landslides.

- Wang H, Gangjun L, Weiya X, Gonghui W. (2005) Gis-based landslide hazard assessment: an overview. *Prog Phys Geog.* 29:548–567.
- Xie M, Esaki T, Cai M. 2004. A time-space based approach for mapping rainfall-induced shallow landslide hazard. *Environ Geol.* 46:840–850.
- Zeze J, Trigo R, Trigo I. 2005. Shallow and deep landslides induced by rainfall in the Lisbon region (Portugal): assessment of relationships with the North Atlantic oscillation. *Nat Hazards Earth Syst Sci.* 5:331–344.
- Zêze JL, Reis E, Garcia R, Oliveira S, Rodrigues ML, Vieira G, Ferreira AB. 2004. Integration of spatial and temporal data for the definition of different landslide hazard scenarios in the area north of Lisbon (Portugal). *Nat Hazards Earth Syst Sci.* 4:133–146.